TDOA Matrices: Algebraic Properties and their Application to Robust Denoising with Missing Data

Jose Velasco, Daniel Pizarro, Javier Macias-Guarasa, *Member, IEEE*, and Afsaneh Asaei, *Member, IEEE*

***Abstract*—Measuring the Time delay of Arrival (TDOA) between a set of sensors is the basic setup for many applications, such as localization or signal beamforming. This paper presents the set of TDOA matrices, which are built from noise-free TDOA measurements. We prove that TDOA matrices are rank-two and have a special SVD decomposition that leads to a compact linear parametric representation. Properties of TDOA matrices are applied in this paper to perform denoising, by finding the TDOA matrix closest to the matrix composed with noisy measurements. The paper shows that this problem admits a closed-form solution for TDOA measurements contaminated with Gaussian noise which extends to the case of having missing data. The paper also proposes a novel robust denoising method resistant to outliers, missing data and inspired in recent advances in robust low-rank estimation. Experiments in synthetic and real datasets show significant improvements of the proposed denoising algorithms in TDOA-based localization, both in terms of TDOA accuracy estimation and localization error.**

***Index Terms*—TDOA estimation, TDOA denoising, skew-symmetric matrices, matrix completion, missing data**

I. Introduction

Time delay of arrival (TDOA) estimation is an essential pre-processing step for multiple applications in the context of sensor array processing, such as multi-channel source localization [1], self-calibration [2] and beamforming [3]. In all cases, performance is directly related to the accuracy of the estimated TDOAs [4].

Estimating TDOA in noisy environments has been subject of study during the last two decades [5]–[7], and is still an active area of research, benefiting from current advances in signal processing and optimization strategies [8]–[11].

Typically, the TDOA between a single pair of sensors is obtained by measuring the peak of the generalized cross-correlation (GCC) of the received signals on each sensor [12], which are assumed to be generated from a single source. Many factors, such as the spectral content of the signal, multipath propagation, and noise contribute to errors in the estimation of the TDOA.

Given a set of sensors, TDOA measurements can be obtained for every possible pair of sensors. This is commonly known as the *full TDOA set* or *spherical set* [13]. This paper studies how to reduce noise and errors from the full TDOA set. The intuition behind this denoising is to exploit redundancy of the full TDOA set. For n sensors, the full set of $n(n-1)/2$ measurements can be represented by $n-1$ values, which are referred to as the *non-redundant set*. This problem has been studied in the past, showing that one can optimally obtain the non-redundant set when TDOA measurements are contaminated with additive Gaussian noise. This is known as the Gauss-Markov estimator [14]. However, in more realistic scenarios errors are not Gaussian and some of the TDOA measurements may contain outliers. In these cases the Gauss-Markov estimator performs poorly.

This paper presents the TDOA matrix, which is created by the arrangement of the full TDOA set inside a skew-symmetric matrix, and studies the algebraic properties of this matrix, showing that it has rank 2 and a SVD decomposition with $n-1$ degrees of freedom.

These algebraic properties are used in this paper to perform denoising under different scenarios, that include the presence of missing TDOA measurements and outliers. These denoising algorithms are tested in the context of speaker localization with microphone arrays, using synthetic and publicly available real datasets. Our denoising algorithms are able to recover accurate TDOA values for high rates of missing data and outliers, significantly outperforming the Gauss-Markov estimator in those cases.

The main contributions of this work are threefold: *i)* Definition of TDOA matrices and their properties. *ii)* A closed-form solution for TDOA denoising for Gaussian noise and the presence of missing data. *iii)* Novel robust-denoising methods for handling additive correlated noise, outliers and missing data.

A. Notation

Real scalar values are represented by lowercase letters (e.g. δ). Vectors are by default arranged column-wise and are represented by lowercase bold letters (e.g. $\mathbf{x}$). Matrices are represented by uppercase bold letters (e.g. $\mathbf{M}$). Upper-case letters are reserved to define vector and set sizes (e.g. vector $\mathbf{x} = (x_1, \cdots, x_N)^\top$ is of size N), and $\mathbf{x}^\top$ denotes transpose of vector $\mathbf{x}$. Calligraphic fonts are reserved to represent generic sets (e.g. $\mathcal{G}$) or functions applied to matrices (e.g. $\mathcal{P}(\mathbf{X})$). The l_2 norm $\|\cdot\|_2$ will be written by default as $\|\cdot\|$ for simplicity, and $\|\cdot\|_F$ is the Frobenius norm, while $|.|$ is reserved to represent absolute values of scalars. $\mathbf{A} \circ \mathbf{B}$ is the hadamard product between $\mathbf{A}$ and $\mathbf{B}$, defined as the entrywise multiplication of the corresponding matrices. $\mathrm{tr}(\cdot)$ is the trace function.

We also define the normalized unitary vector $\hat{\mathbf{1}}$ as $\hat{\mathbf{1}} = (1, \ldots, 1)^\top / \sqrt{n}$, the null vector $\hat{\mathbf{0}}$ as $\hat{\mathbf{0}} = (0, \ldots, 0)^\top$.

J. Velasco, D. Pizarro, and J. Macias-Guarasa are with the Department of Electronics, Escuela Politécnica Superior, University of Alcalá, 28805 Alcalá de Henares, Spain.

A. Asaei is with Idiap Research Institute and also affiliated with École Polytechnique Fédérale de Lausanne, Switzerland.

E-mails: {jose.velasco, pizarro, macias}@depeca.uah.es, afsaneh.asaei@idiap.ch).

Manuscript received Month Day, 2015; revised Month Day, 2015.

Finally, $\mathbb{1} = n\,\hat{\mathbf{1}}\,\hat{\mathbf{1}}^\top$ is a $n \times n$ matrix with all elements equal to 1, $\mathbf{D_x}$ is a $n \times n$ diagonal matrix where its main diagonal is the vector $\mathbf{x}$, and $\mathbf{I}$ is the identity matrix.

B. Paper Structure

The rest of the paper is distributed as follows. Section II describes related work. In section IV TDOA matrices are described along with a derivation of their properties. TDOA denoising in the white noise case is addressed in section V, also providing a closed-form solution. In sections VI and VII we propose algorithms for robust handling of noise and missing data, respectively, and in section VIII we combine them. We also provide an extensive experimentation to validate the proposed algorithms using both synthetic (Section IX) and real data (Section X). Finally, conclusions are drawn in section XI.

II. Related Work

TDOA estimation is an essential first step for multiple applications related to localization, self-calibration and beamforming, among others.

TDOA based localization is widely used in radar, sonar and acoustics, since no synchronization between the source and sensor is needed. The TDOA information is combined with knowledge of the sensors' positions to generate a Maximum Likelihood spatial estimator made from hyperbolas intersected in some optimal sense. A linear closed-form solution of the former problem, valid when the TDOA estimation errors are small, is given in [15].

Since knowing the position of sensors is mandatory for localization techniques, some strategies have been also proposed in order to calibrate them using only TDOA measurements. In [2], [16], the TDOA problem is converted in a Time of Arrival (TOA) problem estimating the departure time of signals. Then, self-calibration techniques for TOA can be employed. The main drawback of this approach is that the conversion step from TDOA to TOA is very sensitive to outliers and correlated noise.

A precise TDOA estimation is also critical for beamforming techniques and its applications. In [3], for example, additional steps are proposed for selecting the appropriate TDOA value among the correlation peaks, and also dealing with TDOA outliers. These steps include a Viterbi decoding based algorithm which maximizes the continuity of the estimation in several frames, but their approach is mainly empirical, not attempting to benefit from the redundancy of the TDOA measurements.

Hence, an accurate estimation of TDOA is essential for a good performance of any of the former applications based in these measurements.

Typically, when only two sensors are employed, the peak of the generalized cross-correlation (GCC) function of the signals of two sensors is a good estimator for the TDOA, for reasonable noise and reverberation levels [12].

When more than two sensors are used ($n > 2$), there are $n(n-1)/2$ different TDOA measurements from all possible pairs of sensors, forming the *full TDOA set* or *spherical set* [13]. However, all those TDOA measurements are redundant. In fact, usually one sensor is considered the reference sensor, and only the subset of $n-1$ TDOA measurements which involve that sensor are considered. That *non-redundant set* is the set of measurement used by the majority of TDOA-based positioning algorithms proposed in the literature [15], [17]–[21]. Nevertheless, an optimal (denoised) version of the non-redundant set can be estimated from the redundant set using a Bayesian Linear Unbiased Estimator (BLUE), also known as the Gauss-Markov estimator [14].

A closed-form solution for the BLUE estimator is provided in [22], also proving that it is equal to the standard least squares estimator, and that it reaches the Cramer-Rao lower bound for positioning estimation. However, all the results in that work are based on the assumption of additive Gaussian noise, which is unrealistic in many practical applications [23], and doesn't yield good results when correlated noise is present as consequence, for instance, of multipath propagation. Additionally, the experimental results shown in their work are only applied to synthetic data, thus severely limiting its application in real scenarios.

Since periodicity in correlated signals, coherent noise and multi-path due to reverberation are the major sources of non-Gaussian error in TDOA estimation, different approaches have been proposed to deal with them. A basic method consists in making the GCC function more robust, de-emphasizing the frequency-dependent weighting. The Phase Transform (PHAT) [24] is one example of this procedure which has received considerable attention as the basis of acoustic source localization systems due to its robustness in real world scenarios [25], [26]. Other approaches are based in blind estimation of multi-path (room impulse response) [27] but they need a good initialization to perform well.

Some previous works have also proposed more complicated structures in order to represent TDOA redundancy, while not imposing strong assumptions on the noise distribution. In [28] a representation based in graphs allows to disambiguate if a peak in correlation was generated by the direct path or by reverberation applying an efficient search algorithm among all possible combinations. However, they do not explicitly attempt to provide improved TDOA estimations by exploiting their redundancy. On the other hand, [29] presents and studies a structure based in multivectors, with a tensor notation that allow them to also denoise TDOA estimations. Unfortunately, they still keep the Gaussian noise assumption and the experimental analysis is only based on simulated data. Additionaly, those works do not face the problem of outliers and missing measurements in the TDOA values.

Also different matrix representations have been used in the bibliography regarding TDOA formulation. For example [30] uses a representation slightly different to the TDOA matrices we describe here, but such representation does not have the algebraic properties that TDOA matrices have, and their authors do not address an study in this sense.

So, to the best of our knowledge, there are no previous reported work dealing with improving TDOA estimations by exploiting their redundancy, while not imposing Gaussian noise restrictions, and being able to deal with the presence of outliers and missing measurements. These errors will severely impact the performance of applications based in TDOA measurements. In this paper we show that TDOA matrices are a powerful tool that combined with recent advances in robust low-rank estimation, are able to generate novel solutions for these problems.

III. Problem Statement

Hereafter, we assume only one source located at the position $\mathbf{r} = (r_x, r_y, r_z)^\top$, and n sensors synchronized between them and placed in different positions $\mathbf{s}_i = (s_{ix}, s_{iy}, s_{iz})^\top$, $i \in [1, n]$.

Given this setup, let's assume that the source is emitting an unknown signal $x(t)$. Then, the signal received by the sensor i, $x_i(t)$, is without loss of generality, a delayed and attenuated version of $x(t)$ (direct propagation) in addition to a signal $g_i(t)$ which summarizes all the adverse effects, i.e. noise, interference, multipath, etc. Thus, $x_i(t) = x(t - \tau_i) + g_i(t)$, where $\tau_i = \|\mathbf{r} - \mathbf{s}_i\|_2 / c$ is the time of arrival (TOA) of the signal $x(t)$ at the sensor $\mathbf{s}_i$, being c the velocity of propagation.

Assuming that TOA cannot be estimated directly, the time delay of arrival (TDOA) between the sensors i and j is estimated by correlating the received signals $x_i(t)$ and $x_j(t)$ (typically using the Generalized Cross-Correlation GCC [24]).

IV. TDOA matrices

In this section we define TDOA matrices, and develop their main properties. In a nutshell, given any TDOA matrix $\mathbf{M}$, we show that: *i)* $\mathbf{M}$ is rank 2 (Theorem 1) and *ii)* $\mathbf{M}$ can be decomposed as $\mathbf{M} = \left(\mathbf{x}\,\hat{\mathbf{1}}^\top - \hat{\mathbf{1}}\,\mathbf{x}^\top\right)$ with $\mathbf{x} = \mathbf{M}\,\hat{\mathbf{1}}$ (Theorem 2).

These properties are the foundations of the denoising algorithms that we present in sections V and VI, and the missing data recovery proposal described in section VII, plus their combination described in section VIII.

A. Definition of TDOA matrices

Definition 1. *A TDOA matrix $\mathbf{M}$, is a $(n \times n)$ skew-symmetric matrix where the element (i, j) is the time difference of arrival (TDOA) between the signals arriving at sensor i and sensor j:*

$$\mathbf{M} = \{\Delta\tau_{ij}\} = \begin{pmatrix} 0 & \Delta\tau_{12} & \cdots & \Delta\tau_{1n} \\ \Delta\tau_{21} & 0 & \cdots & \Delta\tau_{2n} \\ \vdots & \vdots & \ddots & \vdots \\ \Delta\tau_{n1} & \Delta\tau_{n2} & \cdots & 0 \end{pmatrix} \tag{1}$$

with

$$\Delta\tau_{ij} = (\tau_i - \tau_j), \tag{2}$$

where τ_i is the time of arrival of the signal $x(t)$ at the sensor $\mathbf{s}_i$.

We will also express $\mathbf{M}$ in terms of its columns as $\mathbf{M} = (\mathbf{m}_1, \mathbf{m}_2, \cdots, \mathbf{m}_n)$, being $\mathbf{m}_i = (\Delta\tau_{1i}, \Delta\tau_{2i}, \ldots, \Delta\tau_{ni})^\top$.

We denote as $\mathcal{M}_T(n)$ to the set of TDOA matrices of size $n \times n$.

Notice that there is a bijection between the full TDOA set and the corresponding TDOA matrix. Nevertheless expressing TDOA measurements as a matrix has important advantages, that we will discover throughout this article.

B. Algebraic properties of TDOA matrices

1) Rank Properties:

Theorem 1. *Let $\mathbf{M} \in \mathcal{M}_T(n)$, then $\mathbf{M}$ is rank 2.*

Proof: The matrix $\mathbf{M}$ can be expressed as:

$$\mathbf{M} = \mathbf{T} - \mathbf{T}^\top, \tag{3}$$

where $\mathbf{T}$ is a rank 1 matrix defined as:

$$\mathbf{T} = \begin{pmatrix} \tau_1 & \cdots & \tau_1 \\ \vdots & \ddots & \vdots \\ \tau_n & \cdots & \tau_n \end{pmatrix}. \tag{4}$$

Applying the well known inequality:

$$\operatorname{rank}(\mathbf{A} + \mathbf{B}) \le \operatorname{rank}(\mathbf{A}) + \operatorname{rank}(\mathbf{B}), \tag{5}$$

we can deduce that $\operatorname{rank}(\mathbf{M}) \le 2$.

Moreover, since the rank of any skew-symmetric matrix must be even, rank 1 is not feasible. So we can conclude that, excepting the case that $\mathbf{M}$ is the zero matrix (trivial case), the rank of $\mathbf{M}$ is 2. This completes the proof. ■

Rank deficiency of TDOA matrices means that their rows and columns are linearly dependent. That is consistent with the fact that, in the noise-free case, the full TDOA set can be generated from the non-redundant set using linear equations [22]. In fact, in a TDOA matrix, the column j is the TDOA non-redundant set when the sensor j is the reference for TDOA measurements.

Lemma 1. *The normalized unitary vector $\hat{\mathbf{1}}$ can be expressed as a linear combination of any two column vectors of $\mathbf{M} \in \mathcal{M}_T(n)$.*

Proof: Indeed, from (1) and (2), given any two column vectors of $\mathbf{M}$, namely $\mathbf{m}_i$ and $\mathbf{m}_j$ with $i \neq j$, the relation:

$$\frac{\mathbf{m}_i - \mathbf{m}_j}{(\tau_j - \tau_i)\sqrt{n}} = \hat{\mathbf{1}} \tag{6}$$

is satisfied. This completes the proof. ■

2) Singular Value Decomposition: Because $\mathbf{M} \in \mathcal{M}_T(n)$ is a skew-symmetric matrix of rank 2, it has the following singular value decomposition (SVD) [31, Supplementary material]:

$$\mathbf{M} = (\hat{\mathbf{u}}_2, -\hat{\mathbf{u}}_1) \begin{pmatrix} \sigma & 0 \\ 0 & \sigma \end{pmatrix} (\hat{\mathbf{u}}_1, \hat{\mathbf{u}}_2)^\top = \sigma\,(\hat{\mathbf{u}}_2, -\hat{\mathbf{u}}_1)\,(\hat{\mathbf{u}}_1, \hat{\mathbf{u}}_2)^\top, \tag{7}$$

where $\hat{\mathbf{u}}_1$ and $\hat{\mathbf{u}}_2$ are orthonormal vectors and $\sigma \ge 0$. Note that the SVD decomposition of $\mathbf{M}$ is not unique. Given any orthogonal 2×2 matrix $\mathbf{R}$, the vectors $(\hat{\mathbf{v}}_1, \hat{\mathbf{v}}_2) = (\hat{\mathbf{u}}_1, \hat{\mathbf{u}}_2)\,\mathbf{R}$ represent also a valid SVD decomposition:

$$\mathbf{M} = \sigma\,(\hat{\mathbf{v}}_2, -\hat{\mathbf{v}}_1)\,(\hat{\mathbf{v}}_1, \hat{\mathbf{v}}_2)^\top = \sigma\,(\hat{\mathbf{u}}_2, -\hat{\mathbf{u}}_1)\,(\hat{\mathbf{u}}_1, \hat{\mathbf{u}}_2)^\top. \tag{8}$$

Among all possible SVD decompositions of $\mathbf{M}$ we show next that there always exists one where $\hat{\mathbf{u}}_1 = \hat{\mathbf{1}}$. This leads to a parametric representation of $\mathbf{M}$ that has important properties that we will exploit later for TDOA denoising.

Theorem 2. *Given $\mathbf{M} \in \mathcal{M}_T(n)$, it admits the following SVD decomposition:*

$$\mathbf{M} = \sigma \left(\hat{\mathbf{u}}, -\hat{\mathbf{1}}\right) \left(\hat{\mathbf{1}}, \hat{\mathbf{u}}\right)^\top \quad \textit{with} \quad \hat{\mathbf{u}} = \frac{\mathbf{M}\,\hat{\mathbf{1}}}{\|\mathbf{M}\,\hat{\mathbf{1}}\|} \quad \sigma = \|\mathbf{M}\,\hat{\mathbf{1}}\| \tag{9}$$

Proof: According to Theorem 1, the column space of $\mathbf{M}$, lies in a linear subspace of rank 2. Besides, lemma 1 states that vector $\hat{\mathbf{1}}$ belongs to such subspace. Therefore, an orthonormal basis of two vectors $\left\{\hat{\mathbf{1}}, \hat{\mathbf{u}}\right\}$ must exist for the column space of $\mathbf{M}$. The vector $\hat{\mathbf{u}} = \mathbf{u}/\|\mathbf{u}\|$ can be calculated by selecting any column, $\mathbf{m}_i$ with $i = 1, \ldots, n$, and applying Gram-Schmidt as follows:

$$\mathbf{u} = \mathbf{m}_i - (\hat{\mathbf{1}}^\top \mathbf{m}_i)\hat{\mathbf{1}}. \tag{10}$$

Operating, we get $\mathbf{u} = (u_1, \cdots, u_n)^\top$, with

$$u_i = \tau_i - \bar{\tau} \quad \text{and} \quad \bar{\tau} = \sum_{j=1}^{n} \tau_j / n. \tag{11}$$

Note that $\mathbf{u}$ has the same value independently of the column chosen in (10).

As $\{\hat{\mathbf{1}}, \hat{\mathbf{u}}\}$ is a basis of the column space of $\mathbf{M}$, there exist two vectors $\mathbf{c}_1$, $\mathbf{c}_2$ such that:

$$\mathbf{M} = (\mathbf{c}_1, \mathbf{c}_2) \left(\hat{\mathbf{1}}, \hat{\mathbf{u}}\right)^\top, \quad \text{with} \quad \mathbf{c}_1 = \mathbf{M}\,\hat{\mathbf{1}} \quad \mathbf{c}_2 = \mathbf{M}\,\hat{\mathbf{u}}. \tag{12}$$

By substituting (11) and (1) into (12), we verify that:

$$\mathbf{c}_1 = \sqrt{n}\,\|\mathbf{u}\|\,\hat{\mathbf{u}} \quad \text{and} \quad \mathbf{c}_2 = -\sqrt{n}\,\|\mathbf{u}\|\,\hat{\mathbf{1}}. \tag{13}$$

As a consequence of (13) we express $\mathbf{M}$ as:

$$\mathbf{M} = \sqrt{n}\;\|\mathbf{u}\| \left(\hat{\mathbf{u}}, -\hat{\mathbf{1}}\right) \left(\hat{\mathbf{1}}, \hat{\mathbf{u}}\right)^\top. \tag{14}$$

Therefore, from (14) we have:

$$\hat{\mathbf{u}} = \frac{\mathbf{M}\,\hat{\mathbf{1}}}{\left\|\mathbf{M}\,\hat{\mathbf{1}}\right\|}, \qquad \sigma = \sqrt{n}\,\|\mathbf{u}\| = \left\|\mathbf{M}\,\hat{\mathbf{1}}\right\|, \tag{15}$$

from which it follows (9). This completes the proof. ∎

Corollary 2.1. *Any $\mathbf{M} \in \mathcal{M}_T(n)$ can be expressed as:*

$$\mathbf{M} = \left(\mathbf{x}\,\hat{\mathbf{1}}^\top - \hat{\mathbf{1}}\,\mathbf{x}^\top\right) \quad , \quad \mathbf{x} = \mathbf{M}\,\hat{\mathbf{1}} \tag{16}$$

The derivation of (16) follows by substitution of $\mathbf{x} = \sigma\hat{\mathbf{u}}$ in (14).

Corollary 2.2. *Vectors $\mathbf{x}$ and $\hat{\mathbf{1}}$ are orthogonal.*

Corollary 2.3. $\mathbf{M}$ *can also be expressed as:*

$$\mathbf{M} = \frac{1}{\sqrt{n}} \left(\mathbf{D}_\mathbf{x}\,\mathbb{1} - \mathbb{1}\,\mathbf{D}_\mathbf{x}\right) \quad , \hat{\mathbf{1}} \perp \hat{\mathbf{x}}, \tag{17}$$

since $\mathbf{x}\,\hat{\mathbf{1}}^\top = \mathbf{D}_\mathbf{x}\,\mathbb{1}/\sqrt{n}$ and $\hat{\mathbf{1}}\,\mathbf{x}^\top = \mathbb{1}\,\mathbf{D}_\mathbf{x}/\sqrt{n}$,

V. TDOA Denoising

In this section we propose a denoising strategy to deal with Gaussian noise in the estimated TDOA measurements, deriving a closed form solution for the proposed optimization problem. This solution is also compared with the Gauss-Markov Estimator.

A. Denoising Strategy

We assume now that each TDOA measurement is contaminated with uncorrelated Gaussian noise $n_{ij} = -n_{ji}$, such that $\Delta\tilde{\tau}_{ij} = \Delta\tau_{ij} + n_{ij}$. Therefore, the measured TDOA matrix $\tilde{\mathbf{M}} = \{\Delta\tilde{\tau}_{ij}\}$ is also a skew-symmetric matrix, sum of a noise-free $\mathbf{M} \in \mathcal{M}_T(n)$ and a skew-symmetric matrix containing noise $\mathbf{N} = \{n_{ij}\}$:

$$\tilde{\mathbf{M}} = \mathbf{M} + \mathbf{N}. \tag{18}$$

Because of the noise, $\tilde{\mathbf{M}} \notin \mathcal{M}_T(n)$ and thus Theorem 1 is no longer satisfied. Consequently, the rank of $\tilde{\mathbf{M}}$ may be higher than two. Nevertheless, we will show that we can take advantage of the structure of TDOA matrices in order to denoise the measured data.

For denoising, we propose finding the closest $\mathbf{M}^* \in \mathcal{M}_T(n)$, to the measured matrix $\tilde{\mathbf{M}}$, in the sense of the Frobenius norm. This approach yields the following convex optimization problem:

$$\mathbf{M}^* = \underset{\mathbf{M} \in \mathcal{M}_T(n)}{\arg\min} \quad \left\|\tilde{\mathbf{M}} - \mathbf{M}\right\|_F^2. \tag{19}$$

B. Closed-Form Solution

Theorem 3. *Problem* (19) *has the following closed form solution:* $\mathbf{M}^* = (\tilde{\mathbf{M}}\,\mathbb{1} + \mathbb{1}\,\tilde{\mathbf{M}})/n$

Proof: From Corollary 2.1, the denoising problem (19) is equivalent to the following constrained optimization problem:

$$\begin{aligned} &\underset{\mathbf{x}}{\text{minimize}} && \left\|\tilde{\mathbf{M}} - \left(\mathbf{x}\,\hat{\mathbf{1}}^\top - \hat{\mathbf{1}}\,\mathbf{x}^\top\right)\right\|_F^2 \\ &\text{subject to} && \hat{\mathbf{1}}^\top \mathbf{x} = 0. \end{aligned} \tag{20}$$

Using the definition of Frobenius norm $\|\mathbf{A}\|_F^2 = \operatorname{tr}(\mathbf{A}\mathbf{A}^\top)$, and trace properties $\operatorname{tr}(\mathbf{AB}) = \operatorname{tr}(\mathbf{BA})$ and $\operatorname{tr}(\mathbf{A}) = \operatorname{tr}(\mathbf{A}^\top)$ we rewrite the cost as:

$$\begin{aligned} &\left\|\tilde{\mathbf{M}} - \left(\mathbf{x}\,\hat{\mathbf{1}}^\top - \hat{\mathbf{1}}\,\mathbf{x}^\top\right)\right\|_F^2 = \\ &= \operatorname{tr}\left(\left[\tilde{\mathbf{M}} - \left(\mathbf{x}\,\hat{\mathbf{1}}^\top - \hat{\mathbf{1}}\,\mathbf{x}^\top\right)\right]\left[\tilde{\mathbf{M}} - \left(\mathbf{x}\,\hat{\mathbf{1}}^\top - \hat{\mathbf{1}}\,\mathbf{x}^\top\right)\right]^\top\right) \\ &= 2\left(\mathbf{x}^\top\mathbf{x} - \mathbf{x}^\top\,\hat{\mathbf{1}}\,\hat{\mathbf{1}}^\top\mathbf{x} - \hat{\mathbf{1}}^\top\,\tilde{\mathbf{M}}^\top\,\mathbf{x} + \hat{\mathbf{1}}^\top\,\tilde{\mathbf{M}}\,\mathbf{x}\right) + \\ &\quad + \operatorname{tr}\left(\tilde{\mathbf{M}}\,\tilde{\mathbf{M}}^\top\right) = f\left(\mathbf{x}; \tilde{\mathbf{M}}\right). \end{aligned} \tag{21}$$

To solve the constrained problem (20) we use the method of Lagrange multipliers, resulting in the following unconstrained equivalent:

$$\mathbf{x}^* = \underset{\mathbf{x},\lambda}{\arg\min}\,\left[\Lambda\left(\mathbf{x};\lambda\right)\right], \tag{22}$$

where λ is the Lagrange multiplier and

$$\Lambda\left(\mathbf{x};\lambda\right) = f\left(\mathbf{x}; \tilde{\mathbf{M}}\right) + \lambda\hat{\mathbf{1}}^\top\mathbf{x}. \tag{23}$$

We find extrema in (23) by taking first derivatives with respect to both $\mathbf{x}$ and λ and solving the following system:

$$\nabla\Lambda\left(\mathbf{x};\lambda\right) = \hat{\mathbf{0}} \Rightarrow \begin{cases} 2\mathbf{x}^\top\left(\mathbf{I} - \hat{\mathbf{1}}\,\hat{\mathbf{1}}^\top\right) + \hat{\mathbf{1}}^\top\left(\tilde{\mathbf{M}} - \tilde{\mathbf{M}}^\top\right) + \lambda\hat{\mathbf{1}}^\top = \hat{\mathbf{0}}^\top \\ \hat{\mathbf{1}}^\top\mathbf{x} = 0 \end{cases}$$

$$\mathbf{x}^* = \frac{\left(\tilde{\mathbf{M}} - \tilde{\mathbf{M}}^\top\right)\hat{\mathbf{1}} - \lambda\hat{\mathbf{1}}}{2}$$
$$\lambda^* = \frac{\hat{\mathbf{1}}^\top\left(\tilde{\mathbf{M}} - \tilde{\mathbf{M}}^\top\right)\hat{\mathbf{1}}}{2\hat{\mathbf{1}}^\top\hat{\mathbf{1}}}. \tag{24}$$

Since $\tilde{\mathbf{M}}$ is skew-symmetric $(\tilde{\mathbf{M}} - \tilde{\mathbf{M}}^\top) = 2\tilde{\mathbf{M}}$. Therefore, (24) becomes:

$$\mathbf{x}^* = \frac{2\tilde{\mathbf{M}}\,\hat{\mathbf{1}} - \lambda\hat{\mathbf{1}}}{2} = \tilde{\mathbf{M}}\,\hat{\mathbf{1}} \tag{25a}$$
$$\lambda = \frac{2\hat{\mathbf{1}}^\top\tilde{\mathbf{M}}\,\hat{\mathbf{1}}}{2\hat{\mathbf{1}}^\top\hat{\mathbf{1}}} = 2\hat{\mathbf{1}}^\top\tilde{\mathbf{M}}\,\hat{\mathbf{1}} = 0. \tag{25b}$$

In (25b) we use the fact that $\hat{\mathbf{1}}^\top\mathbf{A}\,\hat{\mathbf{1}} = 0$ for $\mathbf{A}$ being a skew-symmetric matrix. Also, it is interesting to note from (25a) that $\mathbf{x}^*$ follows the same expression as the one stated in Corollary 2.1 for $\mathbf{x}$ in the noise-free case.

A compact expression for $\mathbf{M}^*$ can be easily derived from (25a) via (16):

$$\mathbf{M}^* = \left(\hat{\mathbf{1}}, \tilde{\mathbf{M}}\,\hat{\mathbf{1}}\right)\left(-\tilde{\mathbf{M}}\,\hat{\mathbf{1}}, \hat{\mathbf{1}}\right)^\top = \tilde{\mathbf{M}}\,\hat{\mathbf{1}}\,\hat{\mathbf{1}}^\top + \hat{\mathbf{1}}\,\hat{\mathbf{1}}^\top\tilde{\mathbf{M}} = = (\tilde{\mathbf{M}}\mathbb{1} + \mathbb{1}\tilde{\mathbf{M}})/n. \tag{26}$$

This completes the proof. ■

C. Equivalence with the Gauss-Markov Estimator

By operating in (26), each element (i, j) of the denoised matrix $\mathbf{M}^*$ is obtained as follows:

$$\mathbf{M}^* = \{\Delta\tau^*_{ij}\} = \left\{\frac{1}{N}\left(\sum_{k=1}^{n}\Delta\tau_{ik} + \Delta\tau_{kj}\right)\right\}. \tag{27}$$

The closed-form in (27) is identical to the one reported in [22, eq.(14)] as the Gauss-Markov estimator of the TDOA measurements, so that all the properties there can be extrapolated to this work.

VI. Robust TDOA Denoising

In some application scenarios, the assumption of uncorrelated white noise made in section V is fully unrealistic. In such cases where noise is correlated and measurements are prone to contain outliers in the TDOA measurements, a better model for the measured matrix is:

$$\tilde{\mathbf{M}} = \mathbf{M} + \mathbf{N} + \mathbf{S}, \tag{28}$$

where $\mathbf{M} \in \mathcal{M}_T(n)$, $\mathbf{N}$ is a skew-symmetric matrix containing Gaussian noise, much like in (18), and the new matrix $\mathbf{S}$ models the addition of all the outliers. Since the number of outliers is usually small as compared with the number of measurements, we will assume $\mathbf{S}$ to be sparse and unknown.

In order to denoise $\tilde{\mathbf{M}}$, we propose solving the following optimization problem, finding both matrices $\mathbf{M}$ and $\mathbf{S}$:

$$\begin{aligned} \underset{\mathbf{M},\mathbf{S}}{\text{minimize}} \quad & \left\|\tilde{\mathbf{M}} - \mathbf{M} - \mathbf{S}\right\|_F^2 \\ \text{subject to} \quad & \mathbf{M} \in \mathcal{M}_T(n) \\ & \text{card}(\mathbf{S}) < 2k, \end{aligned} \tag{29}$$

where k is the maximum number of outliers supposed to be present in the TDOA measurements.

Robust denoising in (29) is a non-convex optimization problem with constraints that are not even differentiable. This kind of optimization problems have been explored in Robust PCA (RPCA) [32] or robust low-rank factorizations such in GoDec [33]. Despite TDOA matrices are low-rank, these algorithms are not well suited here as they do not include all the algebraic constraints in TDOA matrices.

In order to solve (29), we propose an iterative algorithm, inspired in GoDec. It consists of an alternation method in which $\mathbf{M}$ and $\mathbf{S}$ are obtained in turns, with close-form solutions for these two steps (we use a subindex t to denote the iteration count):

$$\begin{cases} \mathbf{M}_t = \underset{\mathbf{M}\in\mathcal{M}_T(n)}{\arg\min} & \left\|\tilde{\mathbf{M}} - \mathbf{M} - \mathbf{S}_{t-1}\right\|_F^2 \\ \mathbf{S}_t = \underset{\text{card}(\mathbf{S})<2k}{\arg\min} & \left\|\tilde{\mathbf{M}} - \mathbf{M}_t - \mathbf{S}\right\|_F^2 \end{cases} \tag{30}$$

The first sub-problem of (30) is the same as our denoising problem in (19), therefore $\mathbf{M}_t$ can be updated via (26). Then, $\mathbf{S}_t$ is updated via entry-wise hard thresholding of $\tilde{\mathbf{M}} - \mathbf{M}_t$. Thus:

$$\begin{cases} \mathbf{M}_t = \left(\tilde{\mathbf{M}} - \mathbf{S}_{t-1}\right)\hat{\mathbf{1}}\hat{\mathbf{1}}^\top + \hat{\mathbf{1}}\hat{\mathbf{1}}^\top\left(\tilde{\mathbf{M}} - \mathbf{S}_{t-1}\right) \\ \mathbf{S}_t = \mathcal{P}_{2k}\left(\tilde{\mathbf{M}} - \mathbf{M}_t\right) \end{cases} \tag{31}$$

where $\mathcal{P}_l(\mathbf{X})$ is an function which generates a matrix with the same size of $\mathbf{X}$, preserving the l elements of $\mathbf{X}$ with the largest absolute value, and making the rest of elements zero. Note that, since $\mathbf{X}$ is skew symmetric in our application, the result provided by $\mathcal{P}_{2k}(\cdot)$ is also skew symmetric. The convergence to a local minimum of this algorithm is guaranteed in similar circumstances as GoDec [33], as the solutions to both sub-problems in (31) are solved globally.

So, the proposed robust denoising algorithm is:

Require: $\tilde{\mathbf{M}}$, k, ϵ
Ensure: $\mathbf{M} \in \mathcal{M}_T(n)$, $\text{card}(\mathbf{S}) < 2k$,

```
1: M_0 = M̃ ; S_0 = 0 ; t = 0
2: while ||M̃ − M_t − S_t||_F^2 / ||M̃||_F^2 < ε do
3:     t = t + 1
4:     M_t = (M̃ − S_{t−1}) 1̂1̂^⊤ + 1̂1̂^⊤ (M̃ − S_{t−1})
5:     S_t = P_2k(M̃ − M_t)
6: end while
7: return M_t, S_t
```

From now on, we will refer to this algorithm as `Robust DeN`.

VII. Missing Data Recovery

A. Recovery Strategy

In real scenarios, there may be situations where some of the elements of $\tilde{\mathbf{M}}$ might not be available (for instance, due to sensor failure) or even when they are available, there are reasons to avoid using them (for example, due to a priori knowledge of unreliable measurements for some conditions). In such cases, we want to be able to avoid some measurements, thus performing estimations when part of the values in $\tilde{\mathbf{M}}$ are missing.

In this section, we address the TDOA matrix completion problem. We assume that in a measured TDOA matrix $\tilde{\mathbf{M}}$, some of its elements are unknown, an the rest are contaminated with additive Gaussian noise. We take advantage of the redundancy present in TDOA matrices to estimate a complete denoised TDOA matrix including the missing entries.

The matrix completion problem is stated as follows:

$$\mathbf{M}^* = \underset{\mathbf{M}\in\mathcal{M}_T(n)}{\arg\min} \quad \left\| \mathbf{L} \circ \left(\tilde{\mathbf{M}} - \mathbf{M}\right)\right\|_F^2, \tag{32}$$

where $\mathbf{L}$ is a symmetric binary matrix whose element (i, j) is 1 if the TDOA between the sensor i and j is known, being 0 otherwise. For convenience and without loss of generality, the elements on the main diagonal of $\mathbf{L}$ will be set to 1.

Solving (32) is equivalent to finding the full TDOA matrix whose elements best fit the available elements of $\tilde{\mathbf{M}}$. Note that, $\mathbf{L} \circ (\tilde{\mathbf{M}} - \mathbf{M}) = (\tilde{\mathbf{M}}_\mathbf{L} - \mathbf{L} \circ \mathbf{M})$, where $\tilde{\mathbf{M}}_\mathbf{L} = (\mathbf{L} \circ \tilde{\mathbf{M}})$ is the result of setting the unknown elements of $\tilde{\mathbf{M}}$ to zero.

B. Closed-Form Solution

Theorem 4. *The problem* (32) *has the following closed form solution:* $\mathbf{M}^* = \left(\mathbf{D}_\beta + \bar{\mathbf{L}}\right)^{-1} \tilde{\mathbf{M}}_\mathbf{L}\, \mathbb{1} + \mathbb{1}\tilde{\mathbf{M}}_\mathbf{L} \left(\mathbf{D}_\beta + \bar{\mathbf{L}}\right)^{-1}$ *where* $\mathbf{D}_\beta = \left(\mathbf{I} \circ \mathbf{L}\mathbf{L}^\top\right)$ *is a* $n \times n$ *diagonal matrix with* $\boldsymbol{\beta} = \left(n - \bar{\beta}_1, \cdots, n - \bar{\beta}_n\right)^\top = \sqrt{n}\,\mathbf{L}\,\hat{\mathbf{1}}$ *as its main diagonal.* $\bar{\beta}_i$ *is the number of missing measurements with the sensor* i.

Proof: Using Corollary 2.3, problem (32) is rewritten as

$$\begin{aligned} &\underset{\mathbf{x}}{\text{minimize}} && \left\| \tilde{\mathbf{M}}_\mathbf{L} - \frac{\mathbf{L} \circ (\mathbf{D}_\mathbf{x}\mathbb{1} - \mathbb{1}\mathbf{D}_\mathbf{x})}{\sqrt{n}} \right\|_F^2 \\ &\text{subject to} && \hat{\mathbf{1}}^\top \mathbf{x} = 0. \end{aligned} \tag{33}$$

Since $\mathbb{1}$ is the identity element of the hadamard product and $\mathbf{D}_\mathbf{x}$ is a diagonal matrix, we can rewrite (33) as:

$$\begin{aligned} &\underset{\mathbf{x}}{\text{minimize}} && \left\| \tilde{\mathbf{M}}_\mathbf{L} - \frac{(\mathbf{D}_\mathbf{x}\mathbf{L} - \mathbf{L}\mathbf{D}_\mathbf{x})}{\sqrt{n}} \right\|_F^2 \\ &\text{subject to} && \hat{\mathbf{1}}^\top \mathbf{x} = 0. \end{aligned} \tag{34}$$

Operating in a similar manner to (21) we get:

$$\begin{aligned} \left\| \tilde{\mathbf{M}}_\mathbf{L} - \frac{(\mathbf{D}_\mathbf{x}\mathbf{L} - \mathbf{L}\mathbf{D}_\mathbf{x})}{\sqrt{n}} \right\|_F^2 &= \frac{2}{n}\operatorname{tr}\left(\mathbf{D}_\mathbf{x}\mathbf{L}\mathbf{L}^\top\mathbf{D}_\mathbf{x}\right) - \\ - \frac{2}{n}\operatorname{tr}\left(\mathbf{D}_\mathbf{x}\mathbf{L}\mathbf{D}_\mathbf{x}\mathbf{L}\right) &+ \frac{2}{\sqrt{n}}\operatorname{tr}\left(\left[\tilde{\mathbf{M}}_\mathbf{L} - \tilde{\mathbf{M}}_\mathbf{L}^\top\right]\mathbf{D}_\mathbf{x}\mathbf{L}\right) + \\ &+ \operatorname{tr}\left(\tilde{\mathbf{M}}_\mathbf{L}\tilde{\mathbf{M}}_\mathbf{L}^\top\right). \end{aligned} \tag{35}$$

Using the identity $\mathbf{x}^* \left(\mathbf{A} \circ \mathbf{B}\right)\mathbf{y} = \operatorname{tr}\left(\mathbf{D}_\mathbf{x}{}^*\mathbf{A}\mathbf{D}_\mathbf{y}\mathbf{B}^\top\right)$ we get:

$$\begin{aligned} \left\| \tilde{\mathbf{M}}_\mathbf{L} - \frac{(\mathbf{D}_\mathbf{x}\mathbf{L} - \mathbf{L}\mathbf{D}_\mathbf{x})}{\sqrt{n}} \right\|_F^2 &= \frac{2}{n}\mathbf{x}^\top\left(\mathbf{I} \circ \mathbf{L}\mathbf{L}^\top\right)\mathbf{x} \\ - \frac{2}{n}\mathbf{x}^\top\left(\mathbf{L} \circ \mathbf{L}^\top\right)\mathbf{x} &+ 2\,\hat{\mathbf{1}}^\top\left(\left[\tilde{\mathbf{M}}_\mathbf{L} - \tilde{\mathbf{M}}_\mathbf{L}^\top\right] \circ L^\top\right)\mathbf{x} + \\ &+ \operatorname{tr}\left(\tilde{\mathbf{M}}_\mathbf{L}\tilde{\mathbf{M}}_\mathbf{L}^\top\right) = g\left(\mathbf{x}; \tilde{\mathbf{M}}, \mathbf{L}\right) \end{aligned} \tag{36}$$

and finally:

$$\begin{aligned} &\left\| \tilde{\mathbf{M}}_\mathbf{L} - \frac{(\mathbf{D}_\mathbf{x}\mathbf{L} - \mathbf{L}\mathbf{D}_\mathbf{x})}{\sqrt{n}} \right\|_F^2 = \\ &\frac{2}{n}\left(\mathbf{x}^\top\mathbf{D}_\beta\,\mathbf{x} - \mathbf{x}^\top\mathbf{L}\,\mathbf{x} + n\,\hat{\mathbf{1}}^\top\left(\tilde{\mathbf{M}}_\mathbf{L} - \tilde{\mathbf{M}}_\mathbf{L}^\top\right)\mathbf{x}\right) + \\ &+ \operatorname{tr}\left(\tilde{\mathbf{M}}_\mathbf{L}\tilde{\mathbf{M}}_\mathbf{L}^\top\right) = g(\mathbf{x}; \tilde{\mathbf{M}}, \mathbf{L}). \end{aligned} \tag{37}$$

It is important to note that equations (21) and (37) are identical when there is no missing data in $\tilde{\mathbf{M}}$ (i.e $\mathbf{L} = \mathbb{1} = n\,\hat{\mathbf{1}}\,\hat{\mathbf{1}}^\top$ and $\mathbf{D}_\beta = n\,\mathbf{I}$).

We use the method of Lagrange multipliers to express (33) as the following unconstrained optimization problem:

$$\Lambda\left(\mathbf{x}; \lambda\right) = g\left(\mathbf{x}; \tilde{\mathbf{M}}, \mathbf{L}\right) + \lambda\hat{\mathbf{1}}^\top\mathbf{x}. \tag{38}$$

By taking derivatives we obtain the following system:

$$\begin{aligned} &\nabla\Lambda\left(\mathbf{x}; \lambda\right) = \hat{\mathbf{0}} \Rightarrow \\ &\begin{cases} \frac{2}{n}\mathbf{x}^\top\left(\mathbf{D}_\beta - \mathbf{L}\right) + \hat{\mathbf{1}}^\top\left(\tilde{\mathbf{M}}_\mathbf{L} - \tilde{\mathbf{M}}_\mathbf{L}^\top\right) + \lambda\hat{\mathbf{1}}^\top = \hat{\mathbf{0}} \\ \hat{\mathbf{1}}^\top\mathbf{x} = 0. \end{cases} \end{aligned} \tag{39}$$

Since $\hat{\mathbf{1}}^\top\mathbf{x} = 0$ implies that $\mathbb{1}\mathbf{x} = 0$, we substitute in (39) obtaining:

$$\frac{2}{n}\left(\mathbf{D}_\beta + \bar{\mathbf{L}}\right)\mathbf{x} = \left(\tilde{\mathbf{M}}_\mathbf{L} - \tilde{\mathbf{M}}_\mathbf{L}^\top\right)\hat{\mathbf{1}} - \lambda\hat{\mathbf{1}}, \tag{40}$$

where $\left(\bar{\mathbf{L}} = \mathbb{1} - \mathbf{L}\right)$ (logical not operator over all elements of $\mathbf{L}$). Note that: $(\mathbf{D}_\beta + \bar{\mathbf{L}})$ is symmetric and, furthermore, $\hat{\mathbf{1}}$ is one of its eigenvectors.

$$\left(\mathbf{D}_\beta + \bar{\mathbf{L}}\right)\hat{\mathbf{1}} = \frac{\boldsymbol{\beta} + \bar{\boldsymbol{\beta}}}{\sqrt{n}} = n\hat{\mathbf{1}}. \tag{41}$$

Therefore, if the two terms of (40) are multiplied on the right by $\hat{\mathbf{1}}^\top$ we get:

$$2\,\hat{\mathbf{1}}^\top\mathbf{x} = \hat{\mathbf{1}}^\top\left(\tilde{\mathbf{M}}_\mathbf{L} - \tilde{\mathbf{M}}_\mathbf{L}^\top\right)\hat{\mathbf{1}} - \lambda. \tag{42}$$

Then applying to (42) the fact that

$$\hat{\mathbf{1}}^\top\mathbf{x} = 0 \quad \text{and} \quad \hat{\mathbf{1}}^\top(\tilde{\mathbf{M}}_\mathbf{L} - \tilde{\mathbf{M}}_\mathbf{L})\hat{\mathbf{1}} = 0, \tag{43}$$

we can conclude that $\lambda = 0$. Thus, the solution of (33) is:

$$\mathbf{x}^* = n\left(\mathbf{D}_\beta + \bar{\mathbf{L}}\right)^{-1}\tilde{\mathbf{M}}_\mathbf{L}\hat{\mathbf{1}}. \tag{44}$$

Finally, the solution of problem (32) can be calculated from (44) using (16):

$$\mathbf{M}^* = \left(\mathbf{D}_\beta + \bar{\mathbf{L}}\right)^{-1}\tilde{\mathbf{M}}_\mathbf{L}\,\mathbb{1} + \mathbb{1}\tilde{\mathbf{M}}_\mathbf{L}\left(\mathbf{D}_\beta + \bar{\mathbf{L}}\right)^{-1} \tag{45}$$

This completes the proof. ∎

From now on, we will refer to this algorithm as MC. It is noteworthy to comment that the matrix $(\mathbf{D}_\beta + \bar{\mathbf{L}})$ contains important information about the recoverability of missing data: if it is full-rank, then the solution of (32) is unique and if $(\mathbf{D}_\beta + \bar{\mathbf{L}})$ is rank-deficient, missing data is not recoverable uniquely without any further assumption.

Furthermore, in the absence of missing data, $n(\mathbf{D}_\beta + \bar{\mathbf{L}})^{-1} = \mathbf{I}$, hence the matrix completion solution in (45) becomes the solution of the denoising problem stated in (26).

VIII. Robust TDOA Denoising with Missing Data

In this section we aim to combine the results of sections VI and VII, addressing the more general case in which both outliers and missing data are considered. Therefore, the problem is a combination of (29) and (32) defined as:

$$\begin{aligned} \underset{\mathbf{M},\mathbf{S}}{\text{minimize}} \quad & \left\| \mathbf{L} \circ \left(\tilde{\mathbf{M}} - \mathbf{M} - \mathbf{S} \right) \right\|_F^2 \\ \text{subject to} \quad & \mathbf{M} \in \mathcal{M}_T(n) \\ & \operatorname{card}(\mathbf{S}) < 2k \\ & \mathbf{S} = \mathbf{L} \circ \mathbf{S}. \end{aligned} \tag{46}$$

In the same way as in section VI, (46) can be solved by alternatively solving the following two subproblems until convergence:

$$\mathbf{M}_t = \underset{\mathbf{M} \in \mathcal{M}_T(n)}{\arg\min} \left\| \mathbf{L} \circ \left(\tilde{\mathbf{M}} - \mathbf{M} - \mathbf{S}_{t-1} \right) \right\|_F^2 \tag{47a}$$

$$\mathbf{S}_t = \underset{\operatorname{card}(\mathbf{S}) < 2k}{\arg\min} \left\| \mathbf{L} \circ \left(\tilde{\mathbf{M}} - \mathbf{M}_t \right) - \mathbf{S} \right\|_F^2 . \tag{47b}$$

The subproblem (47a) is equivalent to the missing data problem solved in section VII but considering $\tilde{\mathbf{M}}_{\mathbf{L}} = (\mathbf{L} \circ \tilde{\mathbf{M}} - \mathbf{S}_{t-1})$. Therefore, according to theorem 4, it has a closed form solution:

$$\begin{aligned} \mathbf{M}_t^* = (\mathbf{D}_\beta + \bar{\mathbf{L}})^{-1} (\mathbf{L} \circ \tilde{\mathbf{M}} - \mathbf{S}_{t-1})\, \mathbb{1} + \\ + \mathbb{1} (\mathbf{L} \circ \tilde{\mathbf{M}} - \mathbf{S}_{t-1}) (\mathbf{D}_\beta + \bar{\mathbf{L}})^{-1}. \end{aligned} \tag{48}$$

Since (47b) is of the same form as the second subproblem in (30), it can also be solved by entry-wise hard thresholding of $\mathbf{L} \circ (\tilde{\mathbf{M}} - \mathbf{M}_t)$.

The following pseudocode summarizes the proposed algorithm for the general case:

Require: $\tilde{\mathbf{M}}$, $\mathbf{L}$, k, ϵ
Ensure: $\mathbf{M} \in \mathcal{M}_T(n)$, $\operatorname{card}(\mathbf{S}) < 2k$,
1: $\mathbf{D}_\beta = \mathbf{I} \circ \mathbf{L}\mathbf{L}^\top$
2: $\mathbf{Q} = (\mathbf{D}_\beta + \bar{\mathbf{L}})^{-1}$
3: $\mathbf{M}_0 = \tilde{\mathbf{M}}$; $\mathbf{S}_0 = 0$; $t = 0$
4: **while** $\|\tilde{\mathbf{M}} - \mathbf{M}_t - \mathbf{S}_t\|_F^2 / \|\tilde{\mathbf{M}}\|_F^2 < \epsilon$ **do**
5: $\quad t = t + 1$
6: $\quad \mathbf{M}_t = \mathbf{Q}(\mathbf{L} \circ \tilde{\mathbf{M}} - \mathbf{S}_{t-1})\, \mathbb{1} + \mathbb{1}(\mathbf{L} \circ \tilde{\mathbf{M}} - \mathbf{S}_{t-1})\mathbf{Q}$
7: $\quad \mathbf{S}_t = \mathcal{P}_{2k}(\tilde{\mathbf{M}} - \mathbf{M}_t)$
8: **end while**
9: **return** $\mathbf{M}_t$, $\mathbf{S}_t$

Note that in line 2 the matrix $\mathbf{Q} = (\mathbf{D}_\beta + \bar{\mathbf{L}})^{-1}$ can be precalculated in order to get an efficient implementation of the algorithm.

From now on, we will refer to this algorithm as `Robust DeN+MC`.

IX. Experiments with Synthetic Data

In this section computer simulations will be used to compare the proposed algorithms with some of the alternatives existing in the state of the art.

For evaluating the proposed algorithms (robust TDOA denoising and TDOA matrix completion), two different metrics will be used:

- The Signal-to-Noise-Ratio SNR [dB] of the non-redundant set referenced to the first sensor $(10 \log(\sum_{i=1}^{n} \|\Delta\tau_{i1}\|^2 / \sum_{i=1}^{n} \|\Delta\tilde{\tau}_{i1} - \Delta\tau_{i1}\|^2))$. This is an application independent metric, that will allow assessing the proposal improvements in the TDOA measurements *per se*.
- The localization error, measured as the average distance between the source ground truth position and the position estimated using any given localization algorithm based on TDOA estimations (such as [15] in our case). This is an application dependent metric, that will allow assessing the actual benefits of the proposal in a real task.

A. Experimental setup

For all the synthetic data experiments, a set of 10 sensors and 1 source were randomly located. Therefore, 45 different TDOA measurements were generated per experiment, with additive independent Gaussian noise and the same variance for all of them.

The sensor locations were uniformly distributed in a cube of 1 meter side, and the source positions were uniformly distributed in a 2 meter side cube. The propagation speed of the signal was set to 343.313 m/s. To increase the statistical significance of the results, they are provided as averages of 20 independent runs.

B. Evaluation of Robust TDOA Denoising

In this first experiment to evaluate the performance of the algorithm proposed in section VI, we also imposed that some TDOA values were outliers. To simulate this, we randomly chose some measurements (between 0 and 10) and replaced them with a zero-mean Gaussian distributed noise, with a standard deviation of 0.1 ms. It is worth mentioning that the outlier values calculated that way are not related at all to the real TDOAs, thus being *true* outliers. The parameter k of the proposed algorithm, which fixes the maximum number of identifiable outliers, was set to 8.

1) SNR Improvements Evaluation: Fig. 1a shows the SNR values for the proposed robust denoising algorithm when modifying the noise standard deviation and the number of outliers, compared with that obtained by the Gauss-Markov estimator (Fig. 1b), and also when only the non redundant set is used, i.e. not using he redundancy of TDOA measurements (Fig. 1c).

As predicted in section V, when no outliers are present, the performance of the proposed algorithm is the same as Gauss-Markov (see the first row in Figs. 1a and 1b), hence it reaches the Cramer-Rao Bound [22], while being much better than using no redundancy. Nevertheless, the proposed algorithm clearly outperforms the other two approaches when outliers are present in the measurements (rows 1 through 10 in the graphics of Fig. 1).

2) Source Localization Improvements Evaluation: The optimized non redundant set provided by the algorithms applied in Section IX-B1 were used in a localization algorithm using [15]. The average localization errors (in mm) are shown in Fig. 2. Again, the proposed robust denoising algorithm

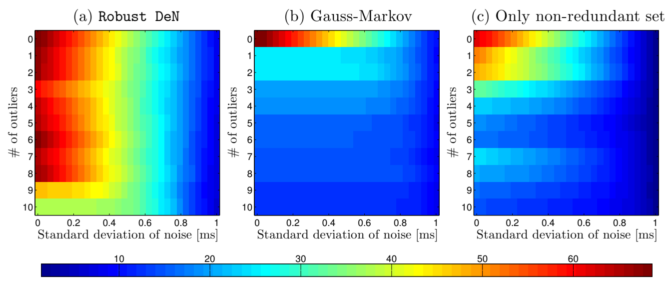

Fig. 1: Robust denoising in synthetic data: SNR in dB (higher is better).

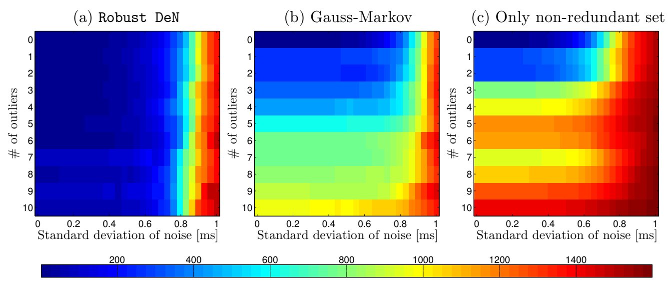

Fig. 2: Robust denoising in synthetic data: Localization error in mm (using [15], lower is better).

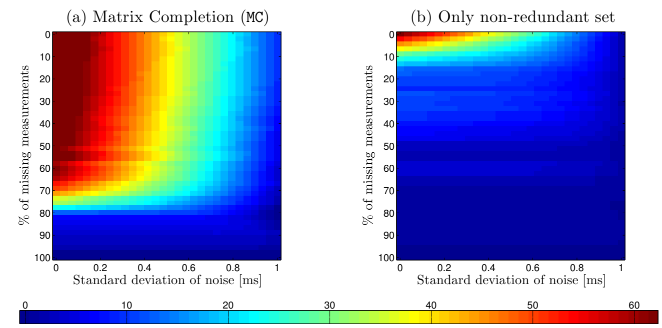

Fig. 3: Missing data recovery in synthetic data: SNR in dB, higher is better.

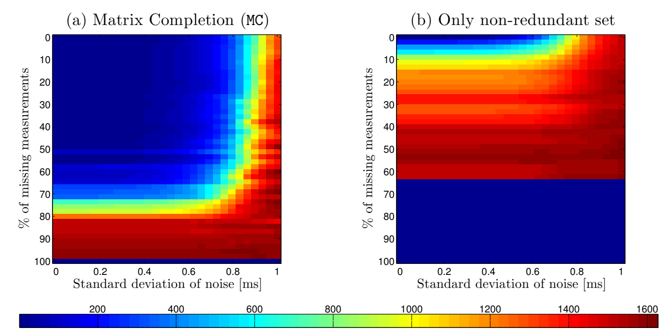

Fig. 4: Missing data recovery in synthetic data: Localization error in mm (using [15], lower is better).

performs as Gauss-Markov when there are no outliers, but is clearly superior when outliers are present.

It is also worth mentioning that the behaviour of the robust denoising keeps the improvements at roughly the same level for increasing number of outliers present, thus validating the ability of the algorithm to pinpoint and eliminate their presence.

C. Evaluation of Missing Data Recovery

In this second experiment, we evaluated the capability of the algorithm proposed in section VII to recover missing values. For our purposes, the missing TDOA measurements were also chosen randomly but, in contrast to the previous experiment, the matrix positions of the missing measurements were known.

Fig. 3 and Fig. 4 show, respectively, the SNR values, and the localization error for the proposed matrix completion algorithm, when modifying the noise standard deviation and the percentage of missing TDOA values in the TDOA matrix, as compared with using only the non-redundant set.

From the figures, it can be clearly seen that the proposed algorithm can take advantage of the knowledge about which measurements were missing, achieving even better results than when the positions of the outliers were unknown. For example, removing 50% of the TDOA measurements implies 24 missing values, much more than the maximum of 10 outliers evaluated in Fig. 1, while keeping good performance.

D. Evaluation of Robust TDOA Denoising with Missing Data

In this third experiment, we evaluated the capability of the algorithm proposed in section VIII to face both outliers and recover missing values.

To provide a wide range of evaluation scenarios, we defined: *i)* Two conditions related to noise, namely *low* and *high*. The former corresponds to a standard deviation of 10^{-3} ms., and the latter to 0.2 ms. *ii)* Two conditions related to the presence of outliers, imposing 2 or 6. *iii)* A variable number of missing TDOA measurements, defined as a percentage of missing TDOA values in the TDOA matrix.

Fig. 5 and Fig. 6 show, respectively, the SNR values, and the localization error for different algorithms, and for different evaluation scenarios.

As it can be seen in Fig. 5a, 6a, 5c and 6c when there are a low number of outliers (2 in this case), the best results are obtained for lower k values. However, when the number of outliers increase, (Fig. 5b, 5d, 6b and 6d, low k values perform worse. So, we can conclude that k must be a number as low as possible, but higher than the number of actual outliers.

Nevertheless, it is worth to observe the behaviour of Fig. 5b, 5d, 6b and 6d (with more outliers) when the percentage of missing data increases. It can be clearly seen that the lines corresponding to different values of k are crossing among them. This seems to indicate that as the missing data percentage increases, the number of outliers that we are able to detect decreases.

Anyway, the results obtained by the `Robust DeN+MC` algorithm outperforms the Gauss-Markov estimator, asymptotically approaching it when the noise is very high. Note also that for high values of noise, the noise and the outliers are practically indistinguishable.

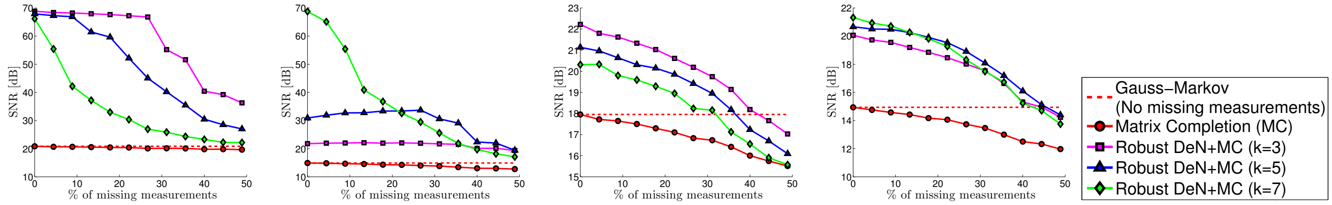

(a) SNR with low noise and 2 outliers (b) SNR with low noise and 6 outliers (c) SNR with high noise and 2 outliers (d) SNR with high noise and 6 outliers

Fig. 5: Algorithm evaluation in synthetic data: SNR in dB.

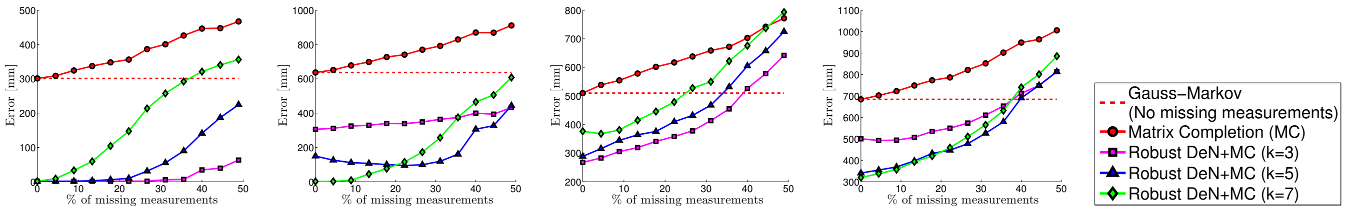

(a) Localization error with low noise and 2 outliers (b) Localization error with low noise and 6 outliers (c) Localization error with high noise and 2 outliers (d) Localization error with high noise and 6 outliers

Fig. 6: Algorithm evaluation in synthetic data: Localization error in mm ([15] is used for source position estimation from the optimized TDOA values).

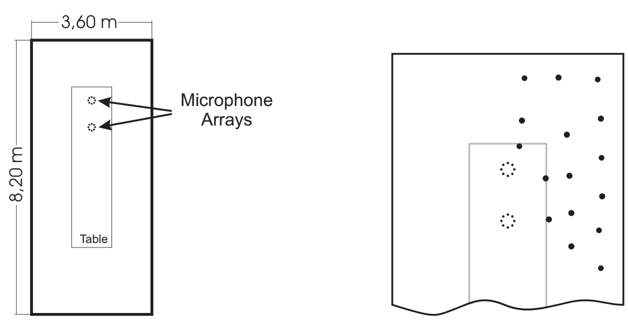

(a) IDIAP room layout showing the centered table, and the microphones arranged in two circular arrays. (b) Positions evaluated in the real data experiments. Only the relevant room section is shown.

Fig. 7: IDIAP Smart Meeting Room: experimental details.

X. Experiments with Real Data

The aim of this section is to evaluate whether the improvements obtained in section IX using synthetic data are actually found in real environments.

A. Experimental Setup

The proposed algorithms have been evaluated using audio recordings from the AV16.3 database [34], an audio-visual corpus recorded in the *Smart Meeting Room* of the IDIAP research institute, in Switzerland.

The IDIAP Meeting Room (shown in Fig. 7) is a $8.2m \times 3.6m \times 2.4m$ rectangular space containing a centrally located $4.8m \times 1.2m$ rectangular table, on top of which two circular microphone arrays of $10cm$ radius are located, each of them composed by 8 microphones. The centers of the two arrays are separated by $80cm$ and the origin of coordinates is located in the middle point between the two arrays. A detailed description of the meeting room can be found in [35].

The audio recordings are synchronously sampled at 16 KHz, and the complete database along with the corresponding annotation files containing the recordings ground truth (3D coordinates of the speaker's mouth) is fully accessible on-line at [36]. It is composed by several sequences from which we are using sequence 01, with a single male speaker generating digit strings in 16 positions (which can be seen as small circles in figure 7b), distributed along the room. The sequence duration accounts for 208 seconds in total, with 823 ground truth frames.

The TDOA measurements $\Delta\tilde{\tau}_{ij}$, from which the measured TDOA matrix $\tilde{\mathbf{M}}$ is built, where estimated using the highest peak of the GCC-PHAT function [24].

As in a real scenario outliers are common but difficult to anticipate or enforce, the sweep over noise levels and the number of outliers that we performed with synthetic data are not feasible. Therefore, in our experiments with real data, we will only provide the SNR values and localization errors obtained after using each algorithm.

B. Evaluation of Robust TDOA Denoising

In this experiment, *all* the microphone pairs have been considered, hence 120 TDOA values have been computed for each frame.

In table I we show an example of the results for the `Robust DeN` with $k = 10$ (set as a reasonable value to face real conditions). As it also happened with synthetic data, in this case the proposed algorithm outperforms the Gauss-Markov estimator, yielding great improvement in both SNR and localization precision.

These results are the baseline for the experiments with missing data described in the next subsection.

C. Evaluation of Robust TDOA Denoising with Missing Data

In the second experiment with real data, we randomly remove a set of TDOA measurements. Fig. 8 shows the ob-

TABLE I: Robust denoising performance in real data

	SNR (dB)	Average Localization error (mm)
`Robust DeN`	27.46	354
Gauss-Markov	23.19	515
Only non-redundant set	17.83	858

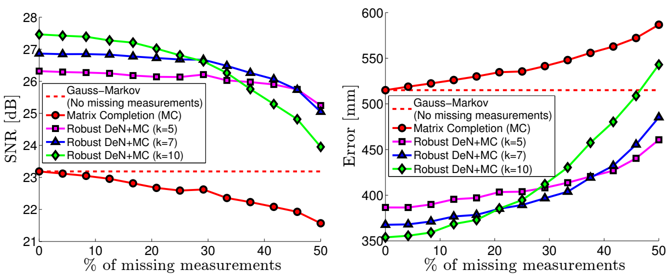

(a) SNR in dB

(b) Localization error in mm (using [15])

Fig. 8: Results for real data with missing TDOA measurements.

tained results. The doted lines correspond to the performance (SNR and localization error) achieved by the Gauss-Markov estimator when there are no missing measurements. The solid lines with circular marks are the results obtained by the matrix completion algorithm (`MC`) described in section VII.

On the other hand, the solid lines with squared/triangular/diamond marks correspond with the results of the `Robust DeN+MC` algorithm presented in section VIII. The different colors/shapes indicate different values of the hyperparameter k.

Fig. 8 highlights the relevance of the proposed robust-denoising algorithm in real-scenarios, with important improvements over the non robust version of our algorithm: higher than 4dB absolute improvement in terms of SNR, and around 30% relative improvement (15 cm absolute) in terms of localization precision.

We again observe that as the percentage of missing data increases, the lines corresponding to different values of k are crossing among them. This behaviour is very similar to that found in the synthetic experiments above (refer to Fig. 5 and Fig 6) for a high number of outliers, what makes us think that this is the case in the real experiment, also serving as a validation for our simulation conclusions.

It is also noteworthy that,in order to get the better result, the maximum number of outliers k should be decreased when the number of missing measurements increases.

XI. Conclusions

This paper has studied the properties of TDOA matrices, showing that they can be effectively used for solving TDOA denoising problems. In particular, the paper has investigated challenging scenarios where the TDOA matrix is contaminated with Gaussian noise, outliers and where a percentage of the measurements are missing. The paper shows that denoising in the presence of Gaussian noise and missing data can be solved in closed-form. This result is important, as it is the basis of an iterative algorithm that can also cope with outliers. The paper has tested the proposed algorithms in the context of acoustic localization using microphone arrays. The experimental results, both on real and synthetic data have shown that our algorithms successfully perform denoising (up to 30% of improvement in localization accuracy) with a high rate of missing data (up to 50%) and outliers. Interestingly, in real datasets our robust denoising algorithm is systematically better than the Gauss-Markov estimator even when there is no missing data and no large outliers are, in principle, contaminating the data. This is an important result as it proves that the assumption of Gaussian noise does not hold in real cases, while our robust model is capable of automatically discard erroneous measurements. As for future work, we plan to further test our denoising algorithms in applications where the position of the sensors is unknown in advance, such in self-localization and beamforming.

References

[1] X. Sheng and Y.-H. Hu, "Maximum likelihood multiple-source localization using acoustic energy measurements with wireless sensor networks," *IEEE Transactions on Signal Processing*, vol. 53, no. 1, pp. 44 – 53, jan. 2005.

[2] Y. Kuang and K. Astrom, "Stratified sensor network self-calibration from tdoa measurements," in *Signal Processing Conference (EUSIPCO), 2013 Proceedings of the 21st European*. IEEE, 2013, pp. 1–5.

[3] X. Anguera, C. Wooters, and J. Hernando, "Acoustic beamforming for speaker diarization of meetings," *Audio, Speech, and Language Processing, IEEE Transactions on*, vol. 15, no. 7, pp. 2011–2022, 2007.

[4] M. Brandstein and D. Ward, Eds., *Microphone Arrays : Signal Processing Techniques and Applications*. Springer, 2001.

[5] G. C. Carter *et al.*, "Special issue on time delay estimation," in *IEEE Trans. Acoust., Speech, Sig. Process.*, G. C. Carter, Ed., Jun 1981, vol. ASSP-29, no. 3, pp. 461 – 624.

[6] J. Chen, J. Benesty, and Y. Huang, "Time delay estimation in room acoustic environments: an overview," *EURASIP Journal on applied signal processing*, vol. 2006, pp. 170–170, 2006.

[7] K. Ho, "Bias reduction for an explicit solution of source localization using tdoa," *Signal Processing, IEEE Transactions on*, vol. 60, no. 5, pp. 2101–2114, 2012.

[8] X. Alameda-Pineda and R. Horaud, "A geometric approach to sound source localization from time-delay estimates," *Audio, Speech, and Language Processing, IEEE/ACM Transactions on*, vol. 22, no. 6, pp. 1082–1095, 2014.

[9] M. Compagnoni, R. Notari, F. Antonacci, and A. Sarti, "A comprehensive analysis of the geometry of tdoa maps in localization problems," *Inverse Problems*, vol. 30, no. 3, p. 035004, 2014.

[10] A. Nouvellet, M. Charbit, F. Roueff, and A. Le Pichon, "Slowness estimation from noisy time delays observed on non-planar arrays," *Geophysical Journal International*, vol. 198, no. 2, pp. 1199–1207, 2014.

[11] B. Huang, L. Xie, and Z. Yang, "Tdoa-based source localization with distance-dependent noises," *Wireless Communications, IEEE Transactions on*, vol. 14, no. 1, pp. 468–480, 2015.

[12] J. DiBiase, H. Silverman, and M. Brandstein, *Microphone Arrays*, 2001, ch. Robust Localization in Reverberant Rooms, pp. 157–180.

[13] B. Yang and J. Scheuing, "A theoretical analysis of 2d sensor arrays for tdoa based localization," in *Acoustics, Speech and Signal Processing, 2006. ICASSP 2006 Proceedings. 2006 IEEE International Conference on*, vol. 4. IEEE, 2006, pp. IV–IV.

[14] W. Hahn and S. Tretter, "Optimum processing for delay-vector estimation in passive signal arrays," *Information Theory, IEEE Transactions on*, vol. 19, no. 5, pp. 608–614, Sep 1973.

[15] Y. Chan and K. Ho, "A simple and efficient estimator for hyperbolic location," *Signal Processing, IEEE Transactions on*, vol. 42, no. 8, pp. 1905–1915, 1994.

[16] M. Pollefeys and D. Nister, "Direct computation of sound and microphone locations from time-difference-of-arrival data." in *ICASSP*, 2008, pp. 2445–2448.

[17] J. O. Smith and J. S. Abel, "Closed-form least-squares source location estimation from range-difference measurements," *Acoustics, Speech and Signal Processing, IEEE Transactions on*, vol. 35, no. 12, pp. 1661–1669, 1987.

[18] M. D. Gillette and H. F. Silverman, "A linear closed-form algorithm for source localization from time-differences of arrival," *Signal Processing Letters, IEEE*, vol. 15, pp. 1–4, 2008.

[19] Y. Weng, W. Xiao, and L. Xie, "Total least squares method for robust source localization in sensor networks using tdoa measurements," *International Journal of Distributed Sensor Networks*, vol. 2011, 2011.

[20] L. Lin, H.-C. So, F. K. Chan, Y. Chan, and K. Ho, "A new constrained weighted least squares algorithm for tdoa-based localization," *Signal Processing*, vol. 93, no. 11, pp. 2872–2878, 2013.

[21] H. Jamali-Rad and G. Leus, "Sparsity-aware multi-source tdoa localization," *Signal Processing, IEEE Transactions on*, vol. 61, no. 19, pp. 4874–4887, 2013.

[22] H. C. So, Y. T. Chan, and F. Chan, "Closed-form formulae for time-difference-of-arrival estimation," *Signal Processing, IEEE Transactions on*, vol. 56, no. 6, pp. 2614–2620, June 2008.

[23] A. Renaux, P. Forster, E. Boyer, and P. Larzabal, "Unconditional maximum likelihood performance at finite number of samples and high signal-to-noise ratio," *Signal Processing, IEEE Transactions on*, vol. 55, no. 5, pp. 2358–2364, 2007.

[24] C. Knapp and G. Carter, "The generalized correlation method for estimation of time delay," *IEEE Transactions on Acoustics, Speech and Signal Processing*, vol. 24, no. 4, pp. 320 – 327, aug 1976.

[25] C. Zhang, D. Florencio, and Z. Zhang, "Why does phat work well in low noise, reverberative environments?" in *Proceedings of ICASSP 2008*, 31 2008-april 4 2008, pp. 2565 –2568.

[26] J. Velasco, C. J. Martín-Arguedas, J. Macias-Guarasa, D. Pizarro, and M. Mazo, "Proposal and validation of an analytical generative model of srp-phat power maps in reverberant scenarios," GEINTRA Research Group, Department of Electronics, University of Alcala, Spain, Tech. Rep. GEINTRA-RR-1-2014, November 2004, http://www.geintra-uah.org/RR-14-01.pdf. [Online]. Available: http://www.geintra-uah.org/RR-14-01.pdf

[27] J. Benesty, "Adaptive eigenvalue decomposition algorithm for passive acoustic source localization," *The Journal of the Acoustical Society of America*, vol. 107, no. 1, pp. 384–391, 2000.

[28] J. Scheuing and B. Yang, "Disambiguation of tdoa estimation for multiple sources in reverberant environments," *Audio, Speech, and Language Processing, IEEE Transactions on*, vol. 16, no. 8, pp. 1479–1489, 2008.

[29] R. Schmidt, "Least squares range difference location," *Aerospace and Electronic Systems, IEEE Transactions on*, vol. 32, no. 1, pp. 234–242, Jan 1996.

[30] P. Annibale, J. Filos, P. Naylor, R. Rabenstein *et al.*, "Tdoa-based speed of sound estimation for air temperature and room geometry inference," *Audio, Speech, and Language Processing, IEEE Transactions on*, vol. 21, no. 2, pp. 234–246, 2013.

[31] G. Ye, D. Liu, I.-H. Jhuo, and S.-F. Chang, "Robust late fusion with rank minimization," in *Computer Vision and Pattern Recognition (CVPR), 2012 IEEE Conference on*. IEEE, 2012, pp. 3021–3028.

[32] E. J. Candès, X. Li, Y. Ma, and J. Wright, "Robust principal component analysis," *Journal of the ACM (JACM)*, vol. 58, no. 3, p. 11, 2011.

[33] T. Zhou and D. Tao, "Godec: Randomized low-rank & sparse matrix decomposition in noisy case," in *in International Conference on Machine Learning*, 2011.

[34] G. Lathoud, J.-M. Odobez, and D. Gatica-Perez, "Av16.3: An audio-visual corpus for speaker localization and tracking," in *Procceedings of the MLMI*, ser. Lecture Notes in Computer Science, S. Bengio and H. Bourlard, Eds., vol. 3361. Springer-Verlag, 2004, pp. 182–195.

[35] D. C. Moore, "The idiap smart meeting room," IDIAP Research Institute, Switzerland, Tech. Rep., November 2004.

[36] G. Lathoud, "Av16.3 dataset," http://www.idiap.ch/dataset/av16-3/, [Last accessed in july 2015].

Jose Velasco received his Telecommunication Engineering Degree and Master Degree in Advanced Electronics, both from Universidad de Alcalá, Spain, in 2010 and 2011 respectively. Currently he is a Ph.D student and his research interests include audio and high dimensional signal coding and processing, with particular emphasis on sparse and low rank representation and modeling.

Daniel Pizarro received both his B.S. and PhD degrees from the University of Alcala in 2003 and 2008 respectively. From 2005 to 2012 he was an Assistant Professor and member of the GEINTRA group at the University of Alcala. From 2012 to 2014 he was an Associate Professor at Universite d'Auvergne and member of ALCoV group. Since 2015 he is Associate Professor at University of Alcala. His research interests are in optimization, Computer Vision, including image registration and the reconstruction of deformable objects and their application to Minimally Invasive Surgery. Daniel Pizarro Pérez has co-authored more than 60 research papers; some in high-impact vision journals such as IEEE PAMI, IJCV, IMAVIS or CVIU and top ranking vision conferences, CVPR, ICCV or ECCV. He has participated in several research projects from public fundings from Spain and Europe and has leaded several technological transfer projects with Spanish companies.

Javier Macias-Guarasa received his Telecommunication Engineering Degree and PhD both from Universidad Politécnica de Madrid, Madrid, Spain, in 1992 and 2001 respectively. From 1990 to 2007 he was a member of the Speech Technology Group and held different teaching positions at Universidad Politécnica de Madrid, currently being Associate Professor in the Department of Electronics at Universidad de Alcalá, Madrid, Spain. In 2003 he was a visiting scientist at at the International Computer Science Institute (ICSI). He has authored or co-authored more than 100 referred papers in the field of Speech Technology and his current research interests are related to speech processing, audiovisual sensor fusion applications in intelligent spaces, and pattern recognition strategies applied to pipeline monitoring systems.

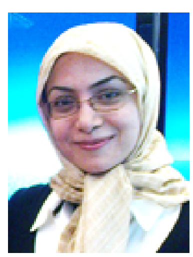

Afsaneh Asaei Afsaneh Asaei received the B.S. degree from Amirkabir University of Technology and the M.S. (honors) degree from Sharif University of Technology, in Electrical and Computer engineering, respectively. She held a research engineer position at Iran Telecommunication Research Center (ITRC) from 2002 to 2008. She then joined Idiap Research Institute in Martigny, Switzerland, and was a Marie Curie fellow on speech communication with adaptive learning training network. She received the Ph.D. degree in 2013 from École Polytechnique Fédérale de Lausanne. Her thesis focused on structured sparsity for multiparty reverberant speech processing, and its key idea was awarded the IEEE Spoken Language Processing Grant. Currently, she is a postdoctoral researcher at Idiap Research Institute. She has served as a guest editor of Speech Communication special issue on Advances in sparse modeling and low-rank modeling for speech processing and co-organized special issues on this topic at HSCMA'2014 and LVA/ICA'2015. Her research interests lie in the areas of signal processing, machine learning, statistics, acoustics, auditory scene analysis and cognition, and sparse signal recovery and acquisition.